Geophysical Research Letters

RESEARCH LETTER
10.1029/2018GL077580

A Statistical Study of Slow-Mode Shocks Observed by MMS in the Dayside Magnetopause

N. K. Walia[1], K. Seki[1], M. Hoshino[1], T. Amano[1], N. Kitamura[2], Y. Saito[2], S. Yokota[3], C. J. Pollock[4,5], B. L. Giles[5], T. E. Moore[5], R. B. Torbert[6], C. T. Russell[7], and J. L. Burch[8]

[1]Department of Earth and Planetary Science, Graduate School of Science, University of Tokyo, Tokyo, Japan, [2]Institute for Space and Astronautical Sciences, JAXA, Sagamihara, Japan, [3]Department of Earth and Space Science, Graduate School of Science, Osaka University Toyonaka Campus, Osaka, Japan, [4]Denali Scientific, Healy, AK, USA, [5]NASA Goddard Space Flight Center, Greenbelt, MD, USA, [6]Physics Department and Space Science Center, University of New Hampshire, Durham, NH, USA, [7]Department of Earth Planetary and Space Sciences, University of California, Los Angeles, CA, USA, [8]Southwest Research Institute, San Antonio, TX, USA

Key Points:
- Seven (14) slow shocks were found on the magnetosphere (magnetosheath) side out of 99 magnetopause crossings with reconnection jets studied
- In the slow shock events, nine rotational discontinuities were observed on the magnetosheath side whereas three were not clearly toward any side
- The smaller the number density ratio of magnetosheath to magnetosphere, the greater the chance to observe magnetosphere slow-mode shocks

Correspondence to:
N. K. Walia,
walia@eps.s.u-tokyo.ac.jp

Citation:
Walia, N. K., Seki, K., Hoshino, M., Amano, T., Kitamura, N., Saito, Y., et al. (2018). A statistical study of slow-mode shocks observed by MMS in the dayside magnetopause. *Geophysical Research Letters*, *45*, 4675–4684. https://doi.org/10.1029/2018GL077580

Received 14 FEB 2018
Accepted 14 MAY 2018
Accepted article online 21 MAY 2018
Published online 31 MAY 2018

Abstract We investigated characteristics of slow-mode shocks in the dayside magnetopause based on Magnetospheric Multiscale observations from September 2015 to February 2017. We analyzed 99 magnetopause crossings with reconnection jets and high time resolution data, out of which 20 crossings showed slow-mode shock signatures. Out of these crossings, one crossing showed slow-mode shock signature on both sides, and the rest had slow-mode shock signatures on one side, six (13) on magnetosphere (magnetosheath). The detection probability of slow-mode shocks in the magnetopause is ~20%, which is greater than that reported in the magnetotail. We also found 12 rotational discontinuities in these slow-mode shock events. The results also show that the observation of magnetosphere side slow-mode shock is favored when the number density ratio of magnetosheath to magnetosphere is small. No clear dependence of the existence of slow-mode shocks on other parameters such as, plasma beta, temperature anisotropy, and jet velocity, was found.

Plain Language Summary When two oppositely directed magnetic field lines come in contact, they break and reconnect releasing large amounts of energy and accelerating particles. This process is called magnetic reconnection. At the dayside interface of the magnetic barrier formed by Earth's intrinsic magnetic field against the plasma flow from the Sun (magnetopause), terrestrial magnetic fields interact with solar magnetic fields through this process. One theory of magnetic reconnection proposes the presence of a structure, called the slow-mode shock, which helps in fast release of energy and acceleration of particles. However, the magnetopause is known to have asymmetric magnetic configuration and only a few observational studies have reported the presence of the slow-mode shock in the magnetopause. Based on observations by the Magnetospheric Multiscale spacecraft in the magnetopause, we found that 20% of the magnetopause crossings with reconnection jets had the slow-mode shock structure. The occurrence frequency is comparable to or a little higher than the symmetric reconnection cases. Their dependence on the number of particles is consistent with previous simulation studies. This study provides substantial evidence that the slow-mode shocks are as common in the asymmetric magnetic reconnection as in the symmetric cases.

1. Introduction

Magnetic reconnection, the process of breaking and reconnecting of magnetic field lines, leads to occurrence of amazing astrophysical phenomena such as magnetospheric storms and solar flares. In Petschek's reconnection model (Petschek, 1964), the outflow region is bound by a pair of slow-mode shocks on both sides with a very small diffusion region. This model deals with symmetric reconnection, and the magnetic field strength and the number density are the same on both sides. It can be well applied to magnetotail reconnection, which is symmetric in nature, but when it comes to magnetopause reconnection, the conditions are far from symmetric. The Levy et al.'s (1964) reconnection model takes into account this asymmetric nature. In this model, they assumed asymmetric magnetic fields and asymmetric number density, though the number density was assumed to be zero on one side. They predicted a rotational discontinuity (RD) and a slow expansion fan instead of slow-mode shocks.

Many MHD simulations have been carried out to study the asymmetric nature of reconnection, especially at the magnetopause (e.g., Biernat et al., 1989; Heyn et al., 1985; Hoshino & Nishida, 1983). Heyn et al. (1985) reported that for two-dimensional reconnection without transverse magnetic field and velocity, they observed a RD and a slow shock (or slow expansion fan) on the magnetosheath side and another slow shock on the magnetosphere side. However, they also noted that if the transverse components are included, then the general structure of the MHD discontinuities observed at the magnetopause should follow the trend of *RD SS* (*F*) *C SS*′(*F*′) *RD*′ (rotational discontinuity followed by a slow-mode shock or slow expansion fan, with contact discontinuity in the middle, followed by another slow-mode shock or slow expansion fan and another rotation discontinuity). The recent studies with MHD and Hall MHD models, with pressure anisotropy (e.g., Hau & Wang, 2016), also report the presence of the same or similar structure.

All these studies point clearly toward the presence of slow-mode shocks in the reconnecting magnetopause at least in the MHD scale, but only two event studies (Sonnerup, Haaland, et al., 2016; Sonnerup, Paschmann, et al., 2016; Walthour et al., 1994) have reported the existence of slow shocks in the magnetopause so far. Walthour et al. (1994) detected the first slow-mode shock using ISEE 2 spacecraft. Slow-mode shock was found to be present only on the magnetosheath side, and a RD was found on the magnetosphere side. Sonnerup, Haaland, et al. (2016) and Sonnerup, Paschmann, et al. (2016) using Time History of Events and Macroscale Interactions during Substorms data found an event with slow-mode shocks at the switch-off limit on both the magnetosphere and magnetosheath side, with a RD on the magnetosphere side. They also reported that the symmetry in their event was established by the cold ions in the magnetosphere side. However, there are a number of reports of detection of slow-mode shocks in the magnetotail (e.g., Eriksson et al., 2004; Feldman et al., 1984; Saito et al., 1995). Saito et al. (1995) did a statistical study using the GEOTAIL satellite in the magnetotail and found that 32 out of 303 (~10%) boundary crossings had slow-mode shocks. The inherent turbulent nature of the magnetopause boundary and low time resolution of earlier missions before Magnetospheric Multiscale (MMS) can be the reason why there are only a few reports of slow-mode shocks in the magnetopause. For a statistical study of slow-mode shocks, we need high time resolution data, which was enabled by MMS.

In this study, we analyzed the magnetopause crossings observed by MMS mission (Burch et al., 2016) to investigate statistical properties of the slow-mode shocks in the dayside magnetopause. We discuss about the detection and analysis method of these slow-mode shocks in section 2. In section 3, observational features of some of the events and the general nature of the observed slow-mode shocks are presented. Section 4 is dedicated to the discussion about these features. We conclude our results in section 5.

2. Instrumentation and Analysis Method

2.1. Data

We used the Fast Plasma Investigation instrument (Pollock et al., 2016) and the Fluxgate Magnetometers (Russell et al., 2016) on board the MMS spacecraft for particle and magnetic field measurements, respectively. For the calculation of accurate ion inertial lengths, the number density for only the slow-mode shock events was also calculated using Hot Plasma Composition Analyzer (Young et al., 2016). The data from these instruments were obtained from the two dayside phases (September 2015 to March 2016 and September 2016 to February 2017), covering all the dayside magnetopause crossings of MMS. First, we used the fast survey data, with the resolution of 4.5 s, to select the southward magnetosheath magnetic field crossings ($B_z < 0$) with an ion jet in the magnetopause ($|V_z| \geq 200$ km/s), in the geocentric solar magnetospheric (GSM) coordinate system. The angle of magnetic field from the z direction, $\cos^{-1}\left(\frac{B_z}{|\boldsymbol{B}|}\right)$, was specified to be $\leq 40°$ on the magnetosphere side and $\geq 120°$ on the magnetosheath side. On the magnetosphere side, plasma beta (β) was specified to be <1, and on the magnetosheath side, β was specified to be >1 and $M_{A(\mathrm{HT})} < 1$ (Alfvén Mach number in the DeHoffmann-Teller frame). We also ensured that all the crossings being studied had burst mode data, which for the ion moments has a resolution of 150 ms, to meet the requirement of high time resolution for our study. With this criterion, we obtained a set of 99 complete magnetopause crossings. The difference between the maximum magnetopause $|V_z|$ and the average magnetosheath $|V_z|$ was checked and was found to be greater than 100 km/s for most of the crossings. The strict constraints on speed of ion jets and $M_{A(\mathrm{HT})}$ could be the reason for reduced number of parent crossings.

2.2. DeHoffmann-Teller Frame and Shock Normal

In order to study shocks, we check the values on the upstream and the downstream of the shock. For the case of magnetopause reconnection, the upstream is magnetosphere or magnetosheath and the downstream is magnetopause. Slow-mode shocks can exist on either side of magnetopause. As an example, shown in Figure 1, the solid blue (red) line is in magnetosphere (magnetosheath) and represents upstream, whereas the dashed line is in the magnetopause and represents downstream. We perform the DeHoffmann-Teller (HT) analysis (Sonnerup et al., 1987) for the full crossing to obtain the frame of reference for our crossings. We use the normal component of the HT velocity (V_{HTn}) as the shock velocity. We note that, here, we are using only one HT frame for the whole crossing (see Sonnerup, Haaland, et al., 2016). The statistical error in the calculation of HT frame is 2 km/s in our study, which is similar to the one used by Sonnerup, Haaland, et al. (2016) (2.5 km/s).

For better visualization of magnetopause crossings, we shift the velocity and magnetic field from GSM to LMN coordinate system. We performed Minimum Variance Analysis (MVA) of the magnetic field values for the whole crossing (Sonnerup & Cahill, 1967). The directions with minimum variance, maximum variance, and intermediate variance are represented as N, L, and M, respectively. These three direction vectors make a right-handed coordinate system, known as the LMN coordinates. Shock normal can be found by using magnetic coplanarity theorem (e.g., Eriksson et al., 2004) or by using MVA (e.g., Sonnerup, Haaland, et al., 2016). For our study, we are using MVA. The direction with minimum variance after doing MVA is chosen as the shock normal. As there can be two shocks on the either side of magnetopause, we divide our full crossing in two halves. One-half contains the magnetosphere side and a part of magnetopause until the point of maximum velocity $|V_L|$ (LMN coordinate), which we will call jet peak, and another half contains the other side of magnetopause, staring from the jet peak to the end of magnetosheath. We do MVA for these two parts separately to obtain two different normal for the two shocks.

2.3. Rankine-Hugoniot Analysis

In order to determine whether there is a shock or not, Rankine-Hugoniot (RH) jump conditions are used (see, e.g., Gurnett & Bhattacharjee, 2005). If each of the RH condition is satisfied, then we can conclude there is a shock. Because of the turbulent nature and rapid motion of magnetopause, for the data analysis purposes, if the RH conditions are satisfied within 30% accuracy, it is considered that a shock is present (e.g., Eriksson et al., 2004; Saito et al., 1995). The six Rankine-Hugoniot relations used correspond to equations (4) to (9) in Eriksson et al. (2004).

Additional six set of set requirements must also be satisfied (e.g., Eriksson et al., 2004) for slow-mode shocks. (1) Plasma pressure (P_p) should increase from upstream to downstream. (2) Magnetic pressure (P_b) should decrease from upstream to downstream. (3) Acute angle of magnetic field with the boundary normal (θ) should decrease from upstream to downstream. (4) Upstream intermediate Alfvén Mach number (M_I) should be less than or equal to 1. (5) Upstream slow-mode magnetosonic Mach number (M_{SM}) should be greater than 1. (6) Downstream M_{SM} should be less than 1.

For slow-mode shock detection, we check the satisfaction of six RH conditions and the six additional conditions (total 12) for all the points in our events. If all these conditions are strictly satisfied, we can say with some certainty that there is a slow-mode shock. When all the slow-mode shock conditions are satisfied for more than one point in our event, then we choose the upstream and downstream that are closest to each other temporally. The downstream intervals are restricted to the jet region (defined by the points that have $|V_z| \geq 200$ km/s, GSM coordinate) in the magnetopause.

The quantities used in the calculation of the 12 slow-mode shock conditions are defined as

$$\boldsymbol{v} = \boldsymbol{v_0} - \mathbf{V_{HT}} \tag{1}$$

where $\boldsymbol{v}$ is the velocity used in RH equations and $\boldsymbol{v_0}$ is the original velocity in the GSM coordinate

$$v_n = \boldsymbol{v}.\boldsymbol{n} \tag{2}$$

where $\boldsymbol{n}$ is the shock normal direction

$$\theta = \cos^{-1}\left(\frac{\boldsymbol{B}.\boldsymbol{n}}{|\boldsymbol{B}|}\right) \tag{3}$$

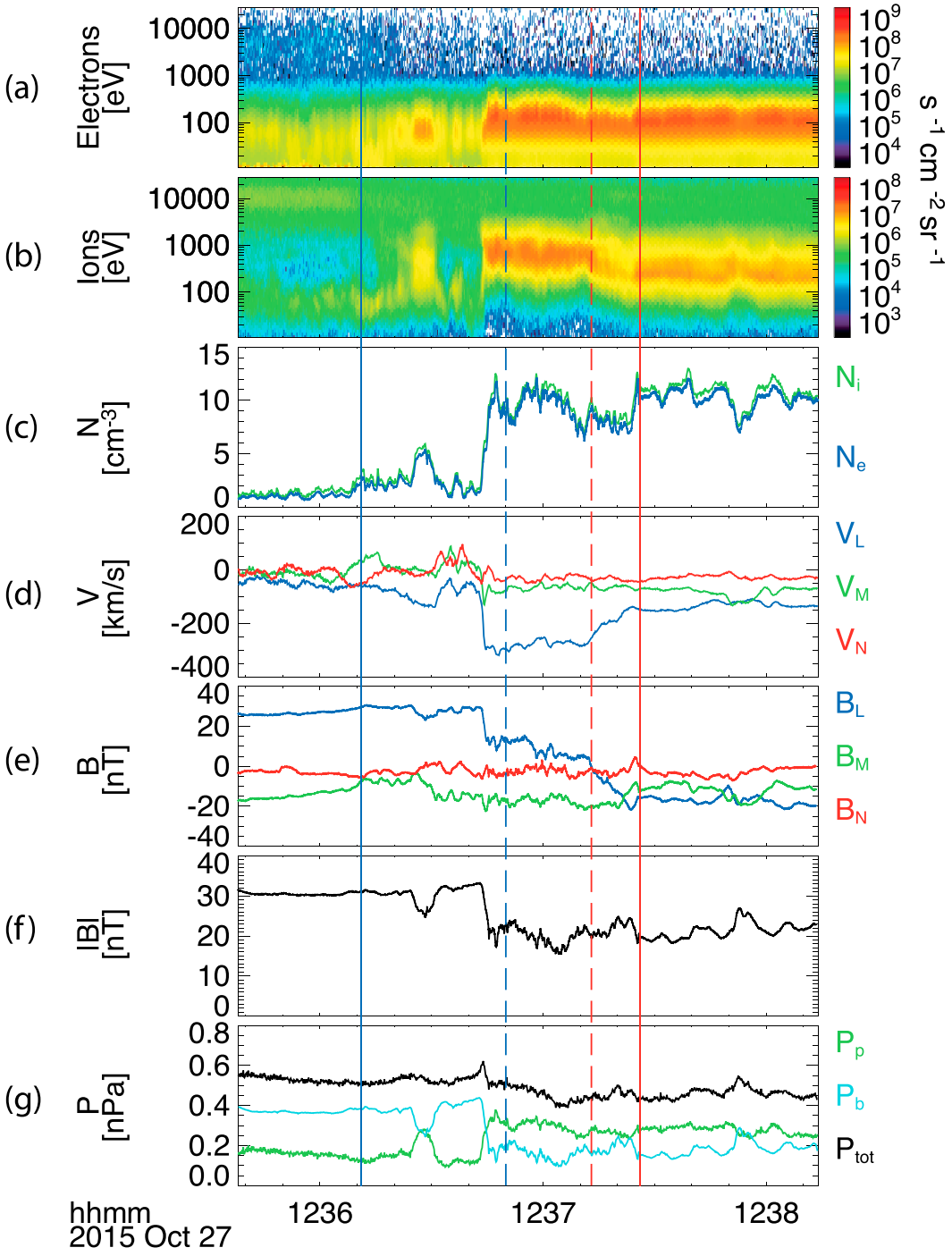

Figure 1. Plot detailing the features of the magnetopause crossing by MMS on 27 October 2015: (a, b) Electron and ion energy-time spectrogram; (c) ion number density (green) and electron number density (blue); (d) ion velocity in LMN coordinate; (e) magnetic field in LMN coordinate; (f) magnetic field magnitude; and (g) plasma pressure (P_p) (green), magnetic pressure (P_b) (cyan), and total pressure (P_{tot}) (black). The solid blue line at 12:36:11 UT marks the upstream of the magnetosphere slow-mode shock, and the dashed blue line at 12:36:50 UT indicates downstream of the same shock. The dashed red line at 12:37:13 UT indicates the downstream of magnetosheath slow-mode shock, and the solid red line at 12:37:26 UT shows upstream of this shock.

Table 1
Twelve Slow-Mode Shock Parameters of the 27 October 2015 Magnetopause Crossing (RH1 Through RH6 Refer to the Rankine-Hugoniot Conditions, Corresponding to Equations (4) to (9) in Eriksson et al., 2004)

	Magnetosphere slow-mode shock		Magnetosheath slow-mode shock	
205-10-27	12:36:11	12:36:50	12:37:26	12:37:13
Parameters	Upstream	Downstream	Upstream	Downstream
P_p (nPa)	0.12	0.28	0.28	0.29
P_b (nPa)	0.38	0.23	0.152	0.151
θ_B (deg)	102.07 (77.93)	104.63 (75.37)	81.73	80.25
M_I	0.52	0.45	0.90	0.66
M_{SM}	1.14	0.62	1.15	0.84
RH1 (10^{-15} kg/m^2 s)	0.22 (79%)	0.28	0.30 (120%)	0.26
RH2 (nPa)	0.51 (98%)	0.52	0.44 (98%)	0.45
RH3 (10^{-3} kg/s^3)	0.03 (100%)	0.03	0.02 (101%)	0.02
RH4 (nT)	6.48 (107%)	6.05	2.81 (85%)	3.30
RH5 (nPa)	0.14 (108%)	0.13	0.06 (88%)	0.07
RH6 (mV/m)	0.89 (70%)	1.27	0.50 (83%)	0.60

$$v_{A=}\frac{|\boldsymbol{B}|}{\sqrt{\rho\mu_0}} \tag{4}$$

where v_A is the Alfvén velocity

$$v_I = v_A\cos\theta \tag{5}$$

$$v_S = \sqrt{\frac{\gamma P_p}{\rho}} \tag{6}$$

$$v_{SM=}\sqrt{\frac{\left(v_S^2+v_A^2\right)-\sqrt{\left(v_S^2+v_A^2\right)^2-4v_S^2v_I^2}}{2}} \tag{7}$$

$$M_I = \left|\frac{v_n}{v_I}\right| \tag{8}$$

$$M_{SM} = \left|\frac{v_n}{v_{SM}}\right| \tag{9}$$

3. Results

3.1. Slow-Mode Shock Observations

When we applied the 12 slow-mode shock conditions to our set of 99 complete magnetopause crossings of MMS 1, obtained over the course of 13 months, 20 crossings showed slow-mode shock signatures. Out of all these crossings, only one event on 27 October 2015 had slow-mode shock signatures on both sides. The remaining 19 crossings had slow-mode shocks only on one side, six on the magnetosphere side, and 13 on the magnetosheath side. We show an overview of the event on 27 October 2015 in Figure 1.

Figure 1c shows a clear jump in number density from magnetosphere to magnetosheath side. A southward directed jet in the magnetopause region, with peak close to 12:36:48 UT, is seen in Figure 1d. In Figure 1e, we can observe the clear transition of B_L from northward direction to southward direction. The rotation of B_M, starting around 12:36:26 UT and reverting back around 12:37:25 UT, could indicate the presence of RD(s). We will later come back to this point. Figure 1g shows a clear increase of P_p from magnetosphere to magnetosheath, while an opposite trend is seen for P_b. One of the interesting features of this event is that it has large guide field and the B_M component of magnetic field never goes to zero as can be seen from Figure 1f.

Table 1 shows the parameters for both the slow-mode shocks. These parameters are similar to the parameters checked by previous studies (e.g., Eriksson et al., 2004). For the first slow-mode shock upstream is the

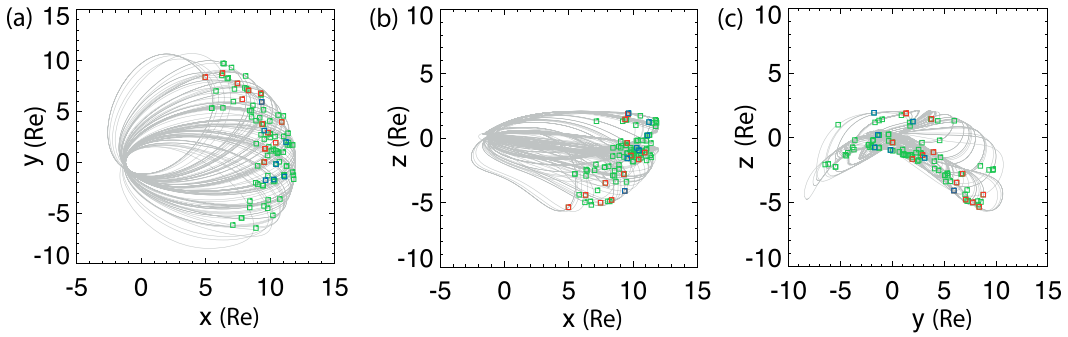

Figure 2. Orbital coverage plots of 99 crossings by MMS in GSM coordinate from 11 September 2015 to 2 February 2017. The gray lines show the orbit of MMS and the squares represent the position of the magnetopause crossing. Red (blue) squares represent the magnetosheath (magnetosphere) slow-mode shock events. The remaining crossings are represented by green squares. MMS = Magnetospheric Multiscale; GSM = geocentric solar magnetospheric.

magnetosphere and downstream is the jet region (in magnetopause), whereas for the second slow-mode shock, upstream is the magnetosheath and downstream is the jet region. We can observe from the table that all the 12 set of conditions required to evaluate the presence of slow-mode shock are well satisfied for both slow-mode shocks in our event (taking into account the 30% accuracy criteria for RH conditions mentioned above).

Another important point to check for slow-mode shocks is whether there is inflow into the shock from upstream, that is, the upstream normal component of velocity ($\mathbf{v}_n$) should have a positive sign for the magnetosphere slow-mode shock and a negative sign for the magnetosheath slow-mode shock. When we apply this additional criterion to our events, we find that 7 out of the 21 slow-mode shocks do not satisfy this condition, including the magnetosphere side slow-mode shock shown in Figure 1. The possible reason behind this can be that the normal velocities might not be determined with very high accuracy for these events as the MVA can sometimes give not so reliable normal direction. But as these events satisfy the 12 slow-mode shock conditions, which have been used in previous studies, we have decided to call these 7 crossings as slow-mode shock crossings as well.

The position of slow-mode shocks in the three GSM coordinates with respect to the total magnetopause crossings is shown in Figure 2. We see that the slow-mode shock events are scattered all over, and there seems to be no clear dependence of the observation of slow shock with respect to its location in the magnetopause. However, from Figure 2a, it does seem that there is no existence of slow-mode shocks in the dawnside region of $y < -2$ Re (Earth radii), even though there are many magnetopause crossings in that region.

3.2. RD Observations

We checked the presence of RDs for the 20 crossings in which we found slow-mode shocks. We checked the magnetic hodograms for all the slow-mode shock events (see, e.g., Neugebauer, 1989; Sonnerup, Haaland, et al., 2016). We found 12 slow-mode shock events to be embedded with RDs. Half of the RDs were merged with the slow-shock structure, whereas half were discrete. By merged, we mean that the rotation seen in hodograms lies within the location of upstream and downstream of shock. Figures 3a and 3b show hodograms for two of the crossings where RDs were found. The clear curve around the $B_M = 0$ line in the B_M versus B_L hodogram (Figures 3a and 3b) and small variance in B_N indicate the presence of RD. We can see for Figure 3 a that the RD is merged with the slow-mode shock as rotation coincides with the location of slow-mode shock, whereas for Figure 3b, it is discrete from the slow-mode shock.

Nine out of the 12 RDs were observed on the magnetosheath side and remaining three could not be regarded to be toward magnetosheath side or magnetosphere side, distinctly. From Figure 3b, we see that the rotation is shown by the red curve rather than the blue one. The red color shows magnetosheath side, and the blue shows magnetosphere side. Hence, we regard this RD as a magnetosheath side RD. Because rotation in Figure 3a is seen in both colors, we regard this RD to be not distinctly toward magnetosphere or magnetosheath side.

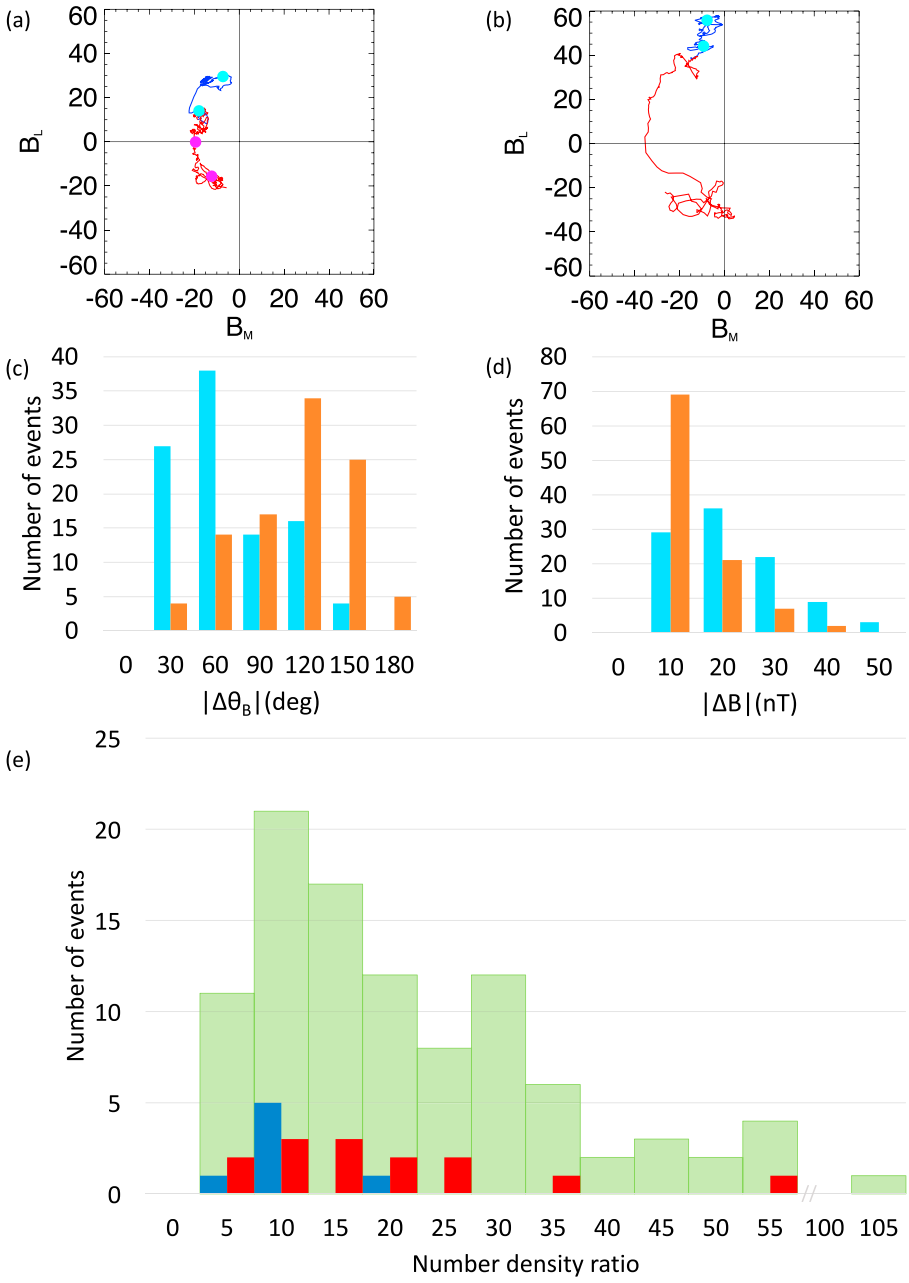

Figure 3. Magnetic hodograms for the slow-mode shock events: (a) 27 October 2015 and (b) 23 November 2016. The circles represent the location of upstream and downstream of slow-mode shocks. The blue hodogram line shows the magnetosphere intervals to jet peak, and the red line shows the intervals from jet peak to the magnetosheath. Histograms for (c) rotation in the LN plane and (d) change in strength of magnetic field across the magnetopause for all the crossings. Cyan bars show the change from magnetosphere to jet region, and the orange bars show the change from jet region to magnetosheath. (e) Histogram of number density ratio of magnetosheath to magnetosphere. Dark blue (red) bars show the number density ratio for magnetosphere (magnetosheath) slow-mode shock events. Green bars show this ratio for all the crossings.

3.3. General Behavior of Magnetosphere to Magnetosheath Crossing

In Figure 3c, θ_B is the angle that magnetic field makes with L direction in the LN plane.

$$\theta_B = \cos^{-1}\left(\frac{B_L}{\left|\sqrt{{B_L}^2+{B_N}^2}\right|}\right) \tag{10}$$

Figure 3c thus represents the change in the rotation of magnetic field ($\Delta\theta_B$) from upstream to downstream. In Figure 3c, the rotation from magnetosphere to jet region as shown by cyan bars is less than the rotation from jet region to magnetosheath, shown by orange bars. This indicates that the rotation of magnetic field occurs toward magnetosheath side.

Figure 3d shows the difference in change of strength of magnetic field (ΔB) on each side. The change in strength of magnetic field is seen to be greater from magnetosphere to jet region (cyan bars) than from magnetosheath to jet region (orange bars). This indicates that the change in strength of magnetic field occurs toward the magnetosphere side.

3.4. Dependence of Slow-Mode Shocks on Magnetosphere and Magnetosheath Parameters

We checked the influence of magnetosphere and magnetosheath parameters such as number density, plasma beta, jet velocity, and temperature anisotropy on the occurrence of slow-mode shocks. No clear dependence on plasma beta, temperature anisotropy, and jet velocity was found. We found dependence with respect to number density ratio, the ratio of number density of magnetosheath to magnetosphere. As shown in Figure 3e, we found that whenever the number density ratio of magnetosheath to magnetosphere is low, there is more chance to see magnetosphere side slow-mode shock (dark blue bars). However, no such dependence on number density was observed for magnetosheath side slow-mode shocks (red bars). We see a similar trend for ion temperature on the magnetosphere side as well. Magnetosphere side slow-mode shocks were seen to be present only in the temperature range of 0.5 to 1.5 keV, whereas the ion temperature of all the crossings varies between 0.3 to 6.2 keV.

4. Discussion

We investigated the magnetopause crossings with high-speed jets to focus on the magnetopause structure with active magnetic reconnection. As explained in section 2.2, we used two normals and one HT frame for checking the presence of 21 slow-mode shocks found from the 99 crossings. Sonnerup, Haaland, et al. (2016) used one HT frame and one normal for their study of slow-mode shocks. Hence, we also tried this criterion of one HT frame and one normal, and we obtained 21 slow-mode shocks from the 99 crossings. We also checked the presence of slow-mode shocks with two normals and two HT frames and obtained 29 slow-mode shocks from 93 boundary crossings. We note that the results with all the three methods are similar. The rest of the crossings, for which we did not observe slow-mode shock (~80%), might have slow expansion fan, intermediate shock, or some other structures.

Slow-shock widths and ion inertial lengths (l_i) were also calculated for each slow-mode shock event (e.g., Sonnerup, Haaland, et al., 2016). The mean slow-shock width for our events was 708 km, and the mean ion inertial length was around 111 km, which gives us the width in terms of ion inertial length as $6l_i$. This width is similar to the width of two slow-mode shocks reported by Sonnerup, Haaland, et al. (2016) ($12l_i$ and $6l_i$ for magnetosphere slow-mode shock and magnetosheath slow-mode shock, respectively).

Our observations also show that in the dayside magnetopause, the rotation of the magnetic field occurs toward the magnetosheath side whereas the change in strength occurs toward the magnetosphere side. Biernat et al. (1989) in their simulation of magnetopause reconnection also found stronger rotation toward the magnetosheath side instead of magnetosphere side. They also note that for asymmetric configuration, which is usually the case, RD on the magnetosphere side is much weaker than magnetosheath RD, and separating it from background fluctuations can be difficult. Our observations are consistent with their simulation results. We can infer that we observed RDs toward magnetosheath side, because the RDs and the rotation on magnetosheath side are much stronger than the magnetosphere side. Walthour et al. (1994) and Sonnerup, Haaland, et al. (2016) had observed RDs on the magnetosphere side instead of magnetosheath side. The three RDs that could not be classified to one side distinctly might correspond to these events. It should be noted that, as Berchem and Russell (1982) pointed out, magnetic field rotation occurs in such a way that the magnetic shear between the magnetosphere magnetic field and the magnetosheath magnetic field is minimum.

The simulation study by Biernat et al. (1989) had also reported the dependence of the observation of slow-mode shocks on the number density ratio between the magnetosheath and the magnetosphere. They found that the chance to observe slow-mode shock increased when the number density ratio decreased. Our statistical results also support this conclusion. Our results show that when the number density ratio of the

magnetosheath to magnetosphere is small, there is an increased chance to observe magnetosphere side slow-mode shocks. The presence of cold ions on the magnetosphere side can cause both a decrease in number density ratio and ion temperature, which is one circumstance to raise the detection probability of the slow-mode shock. Sonnerup, Haaland, et al. (2016) showed an event study that mentions the presence of cold ions and their role in establishing symmetry in their event. This fact is now confirmed by our statistical study. However, it should be noted that if the number density in magnetosheath is very low, then we do not need cold ions to have similar number densities on the magnetosphere and magnetosheath sides. Thus, the low density solar wind is another circumstance to raise the detection probability of the slow-mode shock.

5. Conclusions

We conducted a statistical study of slow-mode shocks in the dayside magnetopause using MMS data from September 2015 to February 2017 that include two dayside phases. In order to investigate the role of slow shocks in magnetopause structure during active reconnection, only the crossings with high speed jets were analyzed. We observed that 20% of the magnetopause crossings studied contained slow-mode shocks. One crossing had slow-mode shocks on both sides, and the rest of the crossings had slow-mode shocks on only one side. Thirteen out of these 19 crossings had slow-mode shocks on the magnetosheath side, and six on the magnetosphere side. Twelve RDs were observed in these slow-mode shock events. Nine RDs were present toward magnetosheath side, whereas three RDs could not be regarded to be toward any side distinctly. As a general structure of the magnetopause crossings, a stronger magnetic field rotation is observed toward the magnetosheath side and stronger change in strength of magnetic field toward magnetosphere side. Magnetosphere side slow-mode shocks were seen to have higher rate of observation when the number density ratio of magnetosheath to magnetosphere was small. Our results provide observational confirmation of the nature of slow-mode shocks derived from previous simulation studies. The results also reveal that the existence of slow-mode shocks in the magnetopause of the terrestrial magnetosphere is as common as in the magnetotail.

Acknowledgments
This work was (partially) supported by Grant-in-Aid for Specially Promoted Research (16H06286) and for Scientific Research (A) 16H02229 by Japan Society for the Promotion of Science (JSPS). The data used in this paper are freely available from the MMS data center: https://lasp.colorado.edu/mms/sdc/public/. We thank the entire MMS team for data access and support.

References

Berchem, J., & Russell, C. T. (1982). Magnetic field rotation through the magnetopause: ISEE 1 and 2 observations. *Journal of Geophysical Research*, *87*, 8139–8148. https://doi.org/10.1029/JA087iA10p08139

Biernat, H. K., Heyn, M. F., Rijnbeek, R. P., Semenov, V. S., & Farrugia, C. J. (1989). The structure of reconnection layers: Application to the Earth's magnetopause. *Journal of Geophysical Research*, *94*, 287–298. https://doi.org/10.1029/JA094iA01p00287

Burch, J. L., Moore, T. E., Torbert, R. B., & Giles, B. L. (2016). Magnetosphere multiscale overview and science objectives. *Space Science Reviews*, *199*(1-4), 5–21. https://doi.org/10.1007/s11214-015-0164-9

Eriksson, S., Øieroset, M., Baker, D. N., Mouikis, C., Vaivads, A., Dunlop, M. W., et al. (2004). Walén and slow-mode shock analyses in the near-Earth magnetotail in connection with a substorm onset on 27 August 2001. *Journal of Geophysical Research*, *109*, A10212. https://doi.org/10.1029/2004JA010534

Feldman, W. C., Schwartz, S. J., Bame, S. J., Baker, D. N., Birn, J., Gosling, J. T., et al. (1984). Evidence for slow-mode shocks in the deep geomagnetic tail. *Geophysical Research Letters*, *11*, 599–602. https://doi.org/10.1029/GL011i006p00599

Gurnett, D. A., & Bhattacharjee, A. (2005). *Introduction to plasma physics: With space and laboratory applications*. Cambridge: Cambridge University Press.

Hau, L.-N., & Wang, B.-J. (2016). Slow shock and rotational discontinuity in MHD and Hall MHD models with anisotropic pressure. *Journal of Geophysical Research, Space Physics*, *121*, 6245–6261. https://doi.org/10.1002/2016JA022722

Heyn, M. F., Biernat, H. K., Semenov, V. S., & Kubyshkin, I. V. (1985). Dayside magnetopause reconnection. *Journal of Geophysical Research*, *90*, 1781–1785. https://doi.org/10.1029/JA090iA02p01781

Hoshino, M., & Nishida, A. (1983). Numerical simulation of the dayside reconnection. *Journal of Geophysical Research*, *88*, 6926–6936. https://doi.org/10.1029/JA088iA09p06926

Levy, R. H., Petschek, H. E., & Siscoe, G. L. (1964). Aerodynamic aspects of the magnetospheric flow. *AIAA Journal*, *2*(12), 2065–2076. https://doi.org/10.2514/3.2745

Neugebauer, M. (1989). The structure of rotational discontinuities. *Geophysical Research Letters*, *16*, 1261–1264. https://doi.org/10.1029/GL016i011p01261

Petschek, H. E. (1964). *NASA special publication 50*, (p. 425). Washington, DC: National Aeronautics and Space Administration, Science and Technical Information Division.

Pollock, C., Moore, T., Jacques, A., Burch, J., Gliese, U., Saito, Y., et al. (2016). Fast plasma investigation for Magnetospheric Multiscale. *Space Science Reviews*, *199*(1-4), 331–406. https://doi.org/10.1007/s11214-016-0245-4

Russell, C. T., Anderson, B. J., Baumjohann, W., Bromund, K. R., Dearborn, D., Fischer, D., et al. (2016). The Magnetospheric Multiscale magnetometers. *Space Science Reviews*, *199*(1-4), 189–256. https://doi.org/10.1007/s11214-014-0057-3

Saito, Y., Mukai, T., Terasawa, T., Nishida, A., Machida, S., Hirahara, M., et al. (1995). Slow-mode shocks in the magnetotail. *Journal of Geophysical Research*, *100*, 23,567–23,581. https://doi.org/10.1029/95JA01675

Sonnerup, B., Haaland, S., Paschmann, G., Phan, T., & Eriksson, S. (2016). Magnetopause reconnection layer bounded by switch-off shocks: 2. Pressure anisotropy. *Journal of Geophysical Research: Space Physics*, *121*, 9940–9955. https://doi.org/10.1002/2016JA023250

Sonnerup, B., Paschmann, G., Haaland, S., Phan, T., & Eriksson, S. (2016). Reconnection layer bounded by switch-off shocks: Dayside magnetopause crossing by THEMIS D. *Journal of Geophysical Research, Space Physics*, *121*, 3310–3332. https://doi.org/10.1002/2016JA022362

Sonnerup, B. U., & Cahill, L. J. Jr. (1967). Magnetopause structure and attitude from Explorer 12 observations. *Journal of Geophysical Research*, *72*, 171–183. https://doi.org/10.1029/JZ072i001p00171

Sonnerup, B. U., Papamastorakis, I., Paschmann, G., & Lühr, H. (1987). Magnetopause properties from AMPTE/IRM observations of the convection electric field: Method development. *Journal of Geophysical Research*, *92*, 12,137–12,159. https://doi.org/10.1029/JA092iA11p12137

Walthour, D. W., Gosling, J. T., Sonnerup, B. U., & Russell, C. T. (1994). Observation of anomalous slow-mode shock and reconnection layer in the dayside magnetopause. *Journal of Geophysical Research*, *99*, 23,705–23,722. https://doi.org/10.1029/94JA01767

Young, D. T., Burch, J. L., Gomez, R. G., De Los Santos, A., Miller, G. P., Wilson, P., et al. (2016). Hot plasma composition analyzer for the Magnetospheric Multiscale mission. *Space Science Reviews*, *199*(1-4), 407–470. https://doi.org/10.1007/s11214-014-0119-6